Novel Hole Transport Materials and their Application for Electrophotography

Nusrallah Jubran[1], Kam Law[1], Zbig Tokarski[1], Ron Moudry[1], and James Baker[1]
Hwan-Koo Lee[2], Valentas Gaidelis[3], Jonas Sidaravicius[3], and Edmundas Montrimas[3]
[1]Samsung Information System America; Digital Printing Solutions Laboratory, Woodbury, Minnesota
[2]Samsung Electronics Co, Suwon, South Korea
[3]Vilnius University, Department of Solid State Electronics, Vilnius, Lithuania
Correspondence on this paper should be e-mailed to njubran@mn.sisa.samsung.com

Abstract

A family of novel dimeric carbazole hydrazones hole transport materials was developed and evaluated for electrophotography. The general structure of the family (shown below) enables us to make several derivatives with different R group substituents on the carbazole and different x linkage groups that connects the two hydrazone moieties

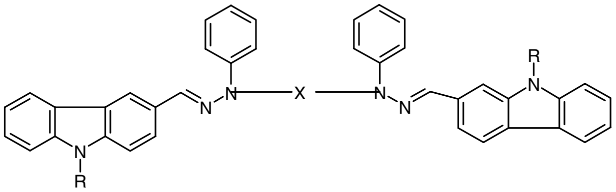

General structure of hole transport material

The synthesis of the hole transport materials was achieved via 4-step reaction sequence: N-alkylation of the carbazole, Vilsmeier reaction followed by reaction with phenylhydrazine. In the final step, the dimer is formed. The total yield of the final product from all 4 steps is ~ 46%. The ^{1}H-NMR spectra of all intermediates along with the final product is in agreement with their structures. The hole drift mobility determined by Time of Flight measurement (TOF), ionization potential and electrophotographic cycling results of these hole transport material will be described

Introduction

There is always a need for new and improved hole transport materials for the electrophotographic market. These hole transport materials play essential role in the electrophotographic process and must fulfill several strict requirements such as, compatibility with other organic photoconductor (OPC) components, ability to transport holes very quickly, not to trap charges, high purity, can be scaled up at affordable price etc…

Experimental

Syntheses

The synthesis of these novel hole transport materials was done in a 4-step reaction sequence.[1] The first step was N-alkylation of carbazole using the phase transfer conditions. The second step is the Vilsmeier reaction followed by the reaction with phenylhydrazine and the final step is the formation of the dimmer. ^{1}H-NMR of all intermediates and final product are in full agreement with their structure.

General Route

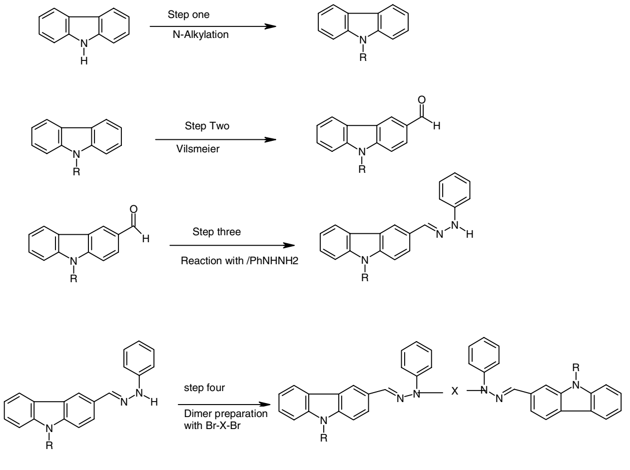

Procedure for Measuring Ionization Potential

Samples for ionization potential Ip measurements were prepared by dissolving charge transport material (CTM) in tetrahydrofuran (THF) and hand-coating on an aluminized polyester substrate that was precision coated with a methylcellulose-based adhesion sub-layer. The role of this sub-layer was to improve adhesion of the CTM layer, to retard crystallization of CTM, and to eliminate the electron photoemission from the Al layer through possible CTM layer defects. No photoemission was detected from the Al through the sub-layer at illumination with up to 6.4 eV quanta energy light. In addition, the adhesion sub-layer was conductive enough to avoid charge accumulation on it during measurements. The thickness of both the sub-layer and CTM layer was ~0.4 µm. No binder material was used with CTM in the preparation of the samples for Ip measurements. In most cases the thin CTM layers are in a meta-stabile amorphous phase, delaying crystallization for several hours, so that measurement of the sample was possible.

The ionization potential was measured by the electron photoemission in air method.[2] The samples were illuminated with monochromatic light from the quartz monochromator with a deuterium lamp source. The power of the incident light beam was $2\text{-}5\cdot10^{-8}$ W. The negative voltage of –300 V was supplied to the sample substrate. The counter-electrode with the 4.5×15 mm^2 slit for illumination was placed at 8 mm distance from the sample surface. The counter-electrode was connected to the input of the BK2-16 type electrometer, working in the open impute regime, for the photocurrent measurement. A 10^{-15} – 10^{-12} amp photocurrent was flowing in the circuit under illumination. The photocurrent, I, was strongly dependent on the incident light photon energy hν. The $I^{0.5}=f(h\nu)$ dependence was plotted. Usually the dependence of the square root of photocurrent on incident light quanta energy is well described by linear relationship near the threshold[3]. The linear part of this dependence was extrapolated to the hν axis and Ip value was determined as the photon energy at the interception point. The ionization potential measurement has an error of ±0.03 eV.

Procedure for Measuring Hole Mobility

Samples for charge carrier mobility measurements and evaluation of electrophotographic parameters were prepared by coating 10 % solutions of the CTM in THF, at the CTM to binder ratio of 4:6 or 5:5, on aluminized polyester substrate. The thickness of the transporting layer varied in the range of 5-10 µm. The mobility for samples with limited solubility could not be measured.

The hole drift mobility was measured by a time of flight technique.[4] Positive corona charging created electric field inside the CTM layer. The charge carriers were generated at the layer surface by illumination with pulses of nitrogen laser (pulse duration was 2 ns, wavelength 337 nm). The layer surface potential decrease as a result of pulse illumination was up to 1-5 % of initial potential before illumination. The capacitance probe that was connected to the wide frequency band electrometer measured the speed of the surface potential decrease dU/dt. The transit time t_t was determined by the change (kink) in the curve of the dU/dt transient in linear or double logarithmic scale. The drift mobility was calculated by the formula $\mu=d^2/U_0\cdot t_t$, where d is the layer thickness and U_0 is the surface potential at the moment of illumination.

Procedure For Measuring Electrostatic Cycling

Extended electrostatic cycling was performed using an in-house designed and developed test bed that tests up to 3 samples strips that are wrapped around a drum. The three coated sample strips, each measuring 50 cm long by 8.8 cm wide, were fastened side-by-side and completely around an aluminum drum (50.3 cm circumference). At least one of the strips was a control sample (US6,140,04 compound 2) that was precision web coated and used as an internal reference point. In this electrostatic cycling tester, the drum rotated at a rate of 8.13 cm / s (3.2ips) and the location of each station in the tester (distance and elapsed time per cycle) is given as:

Electrostatic Test Stations Around The Sample Sheet Wrapped Drum.

Station	Degrees	Total Distance, cm	Total Time, sec
Front erase bar edge	0º	Initial, 0 cm	Initial, 0 s
Erase Bar	0 - 7.2º	0 – 1.0	0 - 0.12
Scorotron	113.1 – 135.3º	15.8 – 18.9	1.94 – 2.33
Laser Strike	161.0º	22.5	2.77
Probe #1	181.1º	25.3	3.11
Probe #2	251.2º	35.1	4.32
Erase bar	360º	50.3	6.19

From the table, the first electrostatic probe (Trek 344 electrostatic meter) is located 0.34 s after the laser strike station and 0.78 s after the scorotron. Also, the second probe (Trek 344 electrostatic meter) is located 1.21 s from the first probe and 1.99 s from the scorotron. All measurements were performed at ambient temperature and relative humidity.

Electrostatic measurements were obtained as a compilation of several tests. The first three diagnostic test (prodstart, VlogE initial, dark decay initial) are designed to evaluate the electrostatic cycling of a new, fresh sample and the last three, identical diagnostic test (prodend, VlogE final, dark decay final) are run after cycling of the sample (longrun).

1. PRODTEST: A charge acceptance and discharge voltage baseline was established by subjecting the samples to corona charging (erase bar always on) for three complete drum revolutions (laser off); discharged with the laser @ 780nm & 600dpi on the forth cycle; completely charged for the next three cycles (laser off);

discharged with only the erase lamp @ 720nm on the eighth cycle (corona and laser off); and, finally, completely charged for the last three cycles (laser off).

2. VLOGE: This test measures the photoinduced discharge of the photoconductor to various laser intensity levels by monitoring the discharge voltage of the belt as a function of the laser power (exposure duration of 50 ns).
3. DARK DECAY: This test measures the loss of charge acceptance with time without laser or erase illumination for 90 seconds and can be used as an indicator of i) the injection of residual holes from the charge generation layer to the charge transport layer, ii) the thermal liberation of trapped charges, and iii) the injection of charge from the surface or aluminum ground plane.
4. LONGRUN: The belt was electrostatically cycled for 100 drum revolutions according to the following sequence per each belt-drum revolution. The belt was charged by the corona, the laser was cycled on and off (80-100° sections) to discharge a portion of the belt and, finally, the erase lamp discharged the whole belt in preparation for the next cycle. The laser was cycled so that the first section of the belt was never exposed, the second section was always exposed, the third section was never exposed, and the final section was always exposed. This pattern was repeated for a total of 100 drum revolutions and the data for every 5th cycle was recorded.
5. After the 100th cycle (long run test), the PRODTEST, VLOGE, DARK DECAY diagnostic tests were run again.

Results and Discussion

Using the general procedure described in the experimental section we were able to make the following novel derivatives

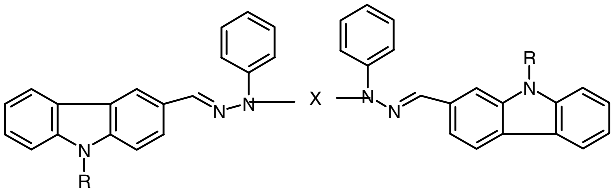

General Structure

CTM1; R = $-CH_2CH_3$; X = $(CH_2)_{10}$
CTM2; R = $-CH_2CH_3$; X = $(CH_2)_5$
CTM3; R = $-CH_2CH_3$; X = $(CH_2)_4$
CTM4; R = $-(CH_2)_6CH_3$; X = $(CH_2)_{10}$
CTM5; R = $-(CH_2)_6CH_3$; X = $(CH_2)_5$
CTM6; R = $-(CH_2)_3C_6H_5$; X = $(CH_2)_5$
CTM7; R = $(CH_2)_3CH_3$; X = $(CH_2)_5$
CTM9; R = $(CH_2)_3CH_3$; X = $(CH_2)_6$
CTM10; R = $(CH_2)_3CH_3$; X = $(CH_2)_8$

In general, the first step gave excellent yield of ~90%, second step gave ~80% yield , third step gave 90% and last step gave ~ 70% yield. ^{1}H-NMR of all intermediates and final product were in full agreement with their structures. The final product was recrystalyzed 3-4 times with activated charcoal and silica gel was added only in the last recrystalysation. Although the ^{1}H-NMR showed pure product after second recrystalyzation, the electrostatic performance was poor and improved only after the third purification. All final products were dried at 70 ^{0}C in a vacuum oven for 7 hours.

The following table provides the mobility values, μ, at the electric field strength, **E**, of $6.4 \cdot 10^5$ V/cm; the Poole-Frenkel coefficient, α, characterizing mobility field dependence on electric field strength, $\mu \sim \exp(\alpha \sqrt{\mathbf{E}})$; and the ionization potential.

CTM	Composition CTM:PC	Hole Mobility μ ($cm^2/V \cdot s$) at $6.4 \cdot 10^5$ V/cm	Poole-Frenkel Coefficient, α $(cm/V)^{1/2}$	Ip (eV)
1	40:60	---	---	5.44
2	40:60	11.0×10^{-6}	0.0054	5.34
4	40:60	4.6×10^{-6}	0.005	5.38
5	40:60	4.5×10^{-6}	0.0051	5.23
7	40:60	3.2×10^{-6}	0.0074	5.4
	50:50	5.7×10^{-6}	0.009	

The following table shows the results from the initial and final prodtest diagnostic tests. The values for the charge acceptance voltage (Vacc, probe #1 average voltage obtained from the third cycle), discharge voltage (Vdis, probe #1 average voltage obtained from the fourth cycle), functional dark decay voltage (Vdd, average voltage difference between probes 1 & 2 obtained from the third cycle), and the residual voltage (Vres, average voltage obtained from the eighth cycle) are reported for the initial and final (post 100th cycle) cycles.

Electrostatic Cycling of Knife-Coated Inverted Dual Layer Constructions.

Cpd	Initial				After 100 cycles			
	Vacc,	Vdd,	Vdis	Vres	Vacc	Vdd	Vdis	Vres
1	526	39	100	43	548	43	113	57
2	495	44	67	22	509	44	73	31
4	639	54	545	434	686	46	612	488
5	546	40	104	42	568	38	127	67
7	513	53	218	119	550	49	257	158
*	568	32	57	16	577	36	62	23

*Comparison compound #2, patent US 6,140,004.

As the electrostatic data indicate these new hole transport materials showed comparable response to that obtained with structure (1) below which showed good applicability for elctrophotography and was disclosed in patents US 6,066,426 and US 6,140,004

The synthesis of these CTMs is much easier than structure (1) and uses less expensive raw materials. This represents a clear economic advantage over structure (1) or other similar derivatives that were mentioned in the above US patents.

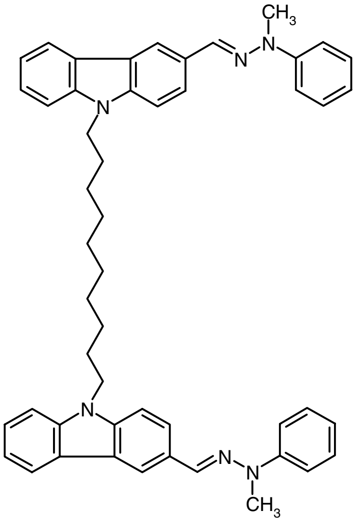

Comparison Structure (1)

Conclusion

The new novel family described above showed comparable electrostatic (ES) data to known hole transport materials that have proven application in electrophotography, and they have clear economic advantage over the structure (1) chemistry because of less expensive raw materials and simpler processes.

Acknowledgement

We are thankful to Professor Dale Russell, Boise State University, Boise, ID for measuring oxidation potential for all hole transport materials[5]

References

1. Charge transport compounds, electrophotographic photoreceptor comprising the same, and electrophotographic imaging apparatus and method" EP # 1202120
2. E. Miyamoto, Y. Yamaguchi, M. Yokoyama, "Ionization Potential of Organic Pigment Film by Atmospheric Photoelectron Emission Analysis", *Electrophotography*, **28**, Nr. 4, p. 364. (1989).
3. M. Cordona, L. Ley. Photoemission in Solids. *Topics in Applied Physics*, **26**, 1-103. (1978).
4. E. Montrimas, V. Gaidelis, A. Pažėra, "The discharge kinetics of negatively charged Se electrophotographic layers," *Lithuanian Journal of Physics*, **6**, p. 569-576 (1966).
5. The oxidation potential of these new CTM range from ~ 0.6 - 1.7 volts. More details on the electrochemistry of these CTMs will be published later.

Biography

Dr. Nusrallah Jubran is currently a staff chemist in Samsung Digital Printing solution Lab, Woodbury, Minnesota. His research activities focus on the development and scale up of novel OPC materials for electrophotography. Prior to joining Samsung, he worked for a period of 13 years with Imation and 3M on several imaging technologies. He published more than 10 US patents and 18 scientific papers.